The non-twist standard map with robust tori

2010 J. Phys. A: Math. Theor. 43 175501

(http://iopscience.iop.org/1751-8121/43/17/175501)

J. Phys. A: Math. Theor. **43** (2010) 175501 (8pp) doi:10.1088/1751-8113/43/17/175501

The non-twist standard map with robust tori

C G L Martins[1], **R Egydio de Carvalho**[1,4], **I L Caldas**[2] **and M Roberto**[3]

[1] Departamento de Estatística, Matemática Aplicada e Computação, Instituto de Geociências e Ciências Exatas, Univ Estadual Paulista-UNESP, 13506-900 Rio Claro, SP, Brazil
[2] Instituto de Física, Universidade de São Paulo, 05315-970 São Paulo, SP, Brazil
[3] Departamento de Física, Instituto Tecnológico da Aeronáutica, 12228-900 São José dos Campos, SP, Brazil

E-mail: carolinegameiro@gmail.com, regydio@rc.unesp.br, ibere@if.usp.br and marisar@ita.br

Received 4 February 2010
Published 14 April 2010
Online at stacks.iop.org/JPhysA/43/175501

Abstract
The non-twist standard map occurs frequently in many fields of science specially in modelling the dynamics of the magnetic field lines in tokamaks. Robust tori, dynamical barriers that impede the radial transport among different regions of the phase space, are introduced in the non-twist standard map in a conservative fashion. The resulting non-twist standard map with robust tori is an improved model to study transport barriers in plasmas confined in tokamaks.

PACS numbers: 05.45.−a, 05.60.Cd, 52.55.Fa, 52.55.−s

(Some figures in this article are in colour only in the electronic version)

1. Introduction

Many techniques have been developed to produce transport barriers in order to increase the confinement time for particles magnetically confined in tokamaks [1–4]. These techniques to implement transport barriers introduce invariant curves on the associated phase space [5]. Dynamical concepts have been applied to interpret the confinement improvement observed in several experiments [6–8]. From the experimental point of view in tokamaks such transport barriers, used to enhance the plasma confinement, can be created by the generation of negative magnetic shear [9–11] as well as the alteration of the radial electric field shear and the poloidal plasma rotation in the vicinity of magnetic islands [12–15].

We propose in this work that the radial transport inside the tokamak plasma can be blocked by creating other barriers, called robust tori (RT) [16–18], which remain intact under the action of any generic perturbation. In fact, from the theoretical point of view, these new barriers constitute insurmountable barriers. The positions of these barriers can be controlled by a parameter. We will develop our strategy by constructing an almost integrable Hamiltonian

[4] Author to whom any correspondence should be addressed.

1751-8113/10/175501+08$30.00

system describing the local dynamics of magnetic field lines on the peripheral region of tokamaks in order to avoid plasma–wall interactions. From this Hamiltonian we will obtain a new sympletic map to describe the dynamics of the magnetic field lines in a poloidal section inside the tokamak.

Our motivation comes from a theoretical approach where the magnetohydrodynamic plasma equilibrium, associated with an integrable Hamiltonian, is described by an analytical solution of the nonlinear Grad–Schlüter–Shafranov equation [19], valid for a large aspect-ratio tokamak approximation and a perturbation using external resonant magnetic coils, called ergodic magnetic limiters (EML) [20, 21], is introduced in order to break the integrability of the field lines inside the tokamak [22–24].

This is achieved by adding to the unperturbed equilibrium Hamiltonian a set of delta-functions perturbations centred at each EML. Due to the impulsive characteristic of this perturbation it is possible to describe the field line dynamics through a two-dimensional map. Depending on whether the frequency profile of the electric current, or on whether the corresponding safety factor, is monotonic or non-monotonic [25–27], the system is classified as a twist or non-twist respectively [28]. In the non-twist case, isochronous resonances [29–31] will emerge in the associate phase space which plays a very important role on the classical transport properties since their non-KAM nature will aid the formation of stickiness [22] when the system is non-integrable due to the existence of curves that encircle the resonances after their reconnection, called *meandering curves* [32].

Besides these stickiness barriers, to improve the plasma confinement described by this system, we suggest that the transport reduction could also be achieved by creating inside the tokamak plasma column invariant barriers, by the creation of RT. These RT will appear when the perturbations are multiplied by a polynomial pre-factor with real roots in such a way that these perturbations are algebraically null over the values of these roots independently of the value of the perturbation parameter. This means that the positions of the RT are theoretically controlled by the values of these roots and all perturbations, with the same pre-factor, vanish on these locations.

Next, we apply this strategy to the mentioned almost integrable Hamiltonian system (describing the local dynamics of magnetic field lines next to the tokamaks wall) and we also derive an analytical map from the field lines equations.

2. Discretization method

The tokamak toroidal geometry naturally leads to the introduction of action-angle variables (J, θ) and to a 1D Hamiltonian. This Hamiltonian models the dynamics of the plasma confinement and it is conveniently decomposed into two terms, one called non-perturbed $H_0(J)$ and another one called perturbation $H_1(J, \theta)$, in such a way that $H(J, \theta) = H_0(J) + \varepsilon H_1(J, \theta)$, with ε a control parameter related to the electric current applied on the EML rings.

The dynamics can be understood looking at the Poincaré section (PS), a transversal plane to the toroidal direction. Successive intersections of a trajectory with the PS allow us to introduce the rotation number, $\alpha(J)$, the angle associated with the discrete dynamics on the PS. Looking at the PS, the motion between two arbitrary intersections, governed by $H_0(J)$, can be described through the map

$$\begin{aligned} J_{n+1} &= J_n \\ \theta_{n+1} &= \theta_n + T\alpha(J_{n+1}), \end{aligned} \tag{1}$$

where n counts the iterations on the PS and T is the period between two consecutive kicks of the perturbation. The choice of J_{n+1} in $\alpha(J)$ is to keep the Jacobian determinant equal to 1. When the system is perturbed by the term $H_1(J,\theta)$, the equations of motion are

$$\begin{aligned} \dot{J} &= -\frac{\partial H}{\partial \theta} = -\varepsilon\frac{\partial H_1}{\partial \theta} = \varepsilon f(J,\theta) \\ \dot{\theta} &= \frac{\partial H}{\partial J} = \frac{\partial H_0}{\partial J} + \varepsilon\frac{\partial H_1}{\partial J} = \alpha(J) + \varepsilon g(J,\theta). \end{aligned} \tag{2}$$

Liouville's theorem [33] establishes that for a conservative system the phase space volume is conserved, which is algebraically described by $\vec{\nabla}\cdot\vec{V} = 0$, that is, the divergence of the velocity vector is null. That condition for a flux reads

$$\frac{\partial f(J,\theta)}{\partial J} = -\frac{\partial g(J,\theta)}{\partial \theta}. \tag{3}$$

Using f and g periodic functions in θ, the map of equation (1) is changed to

$$\begin{aligned} J_{n+1} &= J_n + \varepsilon f(J_{n+1},\theta_n) \\ \theta_{n+1} &= \theta_n + T\ \alpha(J_{n+1}) + \varepsilon g(J_{n+1},\theta_n). \end{aligned} \tag{4}$$

Since the system should preserve area, we will adapt the condition given by equation (3) for the discrete map equations (4) up to $O(\varepsilon)$. This is possible by introducing the generating function, $F_2(J_{n+1},\theta_n)$ [34], for the transformation from iteration n to n+1:

$$F_2(J_{n+1},\theta_n) = J_{n+1}\theta_n + TU(J_{n+1}) + \varepsilon V(J_{n+1},\theta_n), \tag{5}$$

where U and V are auxiliary functions. This choice implies that

$$\begin{aligned} J_n &= \frac{\partial F_2}{\partial \theta_n} = J_{n+1} + \frac{\partial V(J_{n+1},\theta_n)}{\partial \theta_n} \quad \Rightarrow \quad J_{n+1} = J_n - \frac{\partial V(J_{n+1},\theta_n)}{\partial \theta_n} \\ \theta_{n+1} &= \frac{\partial F_2}{\partial J_{n+1}} = \theta_n + T\frac{\partial U(J_{n+1})}{\partial J_{n+1}} + \varepsilon\frac{\partial V(J_{n+1},\theta_n)}{\partial J_{n+1}}. \end{aligned} \tag{6}$$

Comparing these equations with equations (4) leads immediately to the discrete analogous of equation (3):

$$\frac{\partial f}{\partial J_{n+1}} = -\frac{\partial g}{\partial \theta_n}. \tag{7}$$

Hence, the map that we will construct should satisfy equation (7) in order to represent a conservative system.

Looking at equations (2) we can observe that when the non-perturbed Hamiltonian H_0 is a polynomial in the action J of degree greater than 2, the rotation number $\alpha(J)$ and $\alpha(J_{n+1})$ in equations (4) are non-monotonic functions. This is the condition for the map to be non-twist. On the other hand, in order to introduce RT it is necessary that the perturbation H_1 includes a polynomial pre-factor also in the action J. Consequently this pre-factor will appear in the function $f(J_{n+1},\theta_n)$ of the map. Both conditions interfere in the map structure and the degree of the polynomial pre-factor on H_1 will determine the number of RT which will be introduced on the phase space (J,θ).

3. Hamiltonian approach

Due to the toroidal symmetry, the equilibrium Hamiltonian, H_0, does not depend on the toroidal angle φ, which we will choose as the canonical time t. Hence, H_0 is given in terms of the canonical action J, associated with the toroidal normalized flux, and θ the poloidal angle canonically conjugated to J. On the other hand, the perturbing Hamiltonian is a function of J, θ and t, and it will be represented by means of a Fourier series of delta-kicks. We also define the PS in a fixed value of the angle φ.

In order to introduce the quasi-integrable approximation for the plasma confinement we consider the typical Hamiltonian perturbation:

$$H_1(J,\theta) = p(J)\cos(m_0\theta)\sum_{k=-\infty}^{\infty}\delta\left(t-\frac{2\pi k}{N_r}\right), \tag{8}$$

with only one dominant resonant mode m_0 in the poloidal direction. The mode m_0 is determined by the rotation number associated with the perturbing electrical current in the N_r EML placed on the tokamak camera. We have chosen $m_0 = 3$ which creates a resonance 1:3 and the number of EML rings is $N_r = 4$. We have considered $p(J) = 1$ which recovers the usual approach without RT and also the case $p(J) = (J^2{-}a)$ which creates two RT, where the parameter a controls the position of the two RT.

In fact, equation (8) corresponds to a local approximation around a magnetic surface with the action J^*, because when we perturb the equilibrium magnetic field lines with EML rings, many resonant modes would appear besides the chosen main resonant mode, 1:3 in our case. We point out that the single cosine in equation (8) is an approximation of an infinite Fourier expansion in order to avoid the interaction among different resonant modes which would increase the chaotic sea. This approximation allows us to understand the fundamental physics that is occurring on the local approximation, around the resonance 1:3, which could be camouflaged by the chaotic sea if we had considered other resonant modes. This method that we are presenting here will also work even if many resonant modes were acting on the system; RT could surely survive to the perturbations if all of them have a same pre-factor in such way that they would be simultaneously null over RT.

Thus, following [22], we write the unperturbed Hamiltonian H_0 in a near-action variable, $\Delta J = (J{-}J^*)$, as a cubic polynomial which introduces two isochronous resonance chains:

$$H_0(\Delta J) = \frac{\Delta J^2}{2} - \beta\frac{\Delta J^3}{3}, \tag{9}$$

where β is a parameter that measures the non-pendular character of the resonance and it is related to the safety factor in experimental setups in the tokamak TCABR. For the purpose of this work, we set $\beta = 160.15$, which is a little higher than the one used in the experiments. So, the Hamiltonian (9) perturbed with the term (8) written in the near-action ΔJ and quadratic $p(J)$ is given as

$$H(\Delta J,\theta) = \left(\frac{\Delta J^2}{2} - \beta\frac{\Delta J^3}{3}\right) + \varepsilon\left(\Delta J^2 - a\right)\left\{\cos(m_0\theta)\sum_{k=-\infty}^{\infty}\delta\left(t-\frac{2\pi k}{N_r}\right)\right\}. \tag{10}$$

The equations of motion governed by this Hamiltonian are

$$\begin{aligned}\dot{\Delta J} &= -\frac{\partial H}{\partial\theta} = \varepsilon\left(\Delta J^2 - a\right)m_0\sin(m_0\theta)\sum_{k=-\infty}^{\infty}\delta\left(t-\frac{2\pi k}{N_r}\right) = \varepsilon f(\Delta J,\theta),\\ \dot\theta &= \frac{\partial H}{\partial\Delta J} = \left(\Delta J - \beta\Delta J^2\right) + \varepsilon 2\Delta J\cos(m_0\theta)\sum_{k=-\infty}^{\infty}\delta\left(t-\frac{2\pi k}{N_r}\right) = \alpha(\Delta J) + \varepsilon g(\Delta J,\theta),\end{aligned} \tag{11}$$

from where it is possible to see that equations (2) and (3) are satisfied for the variables $(\Delta J, \theta)$.

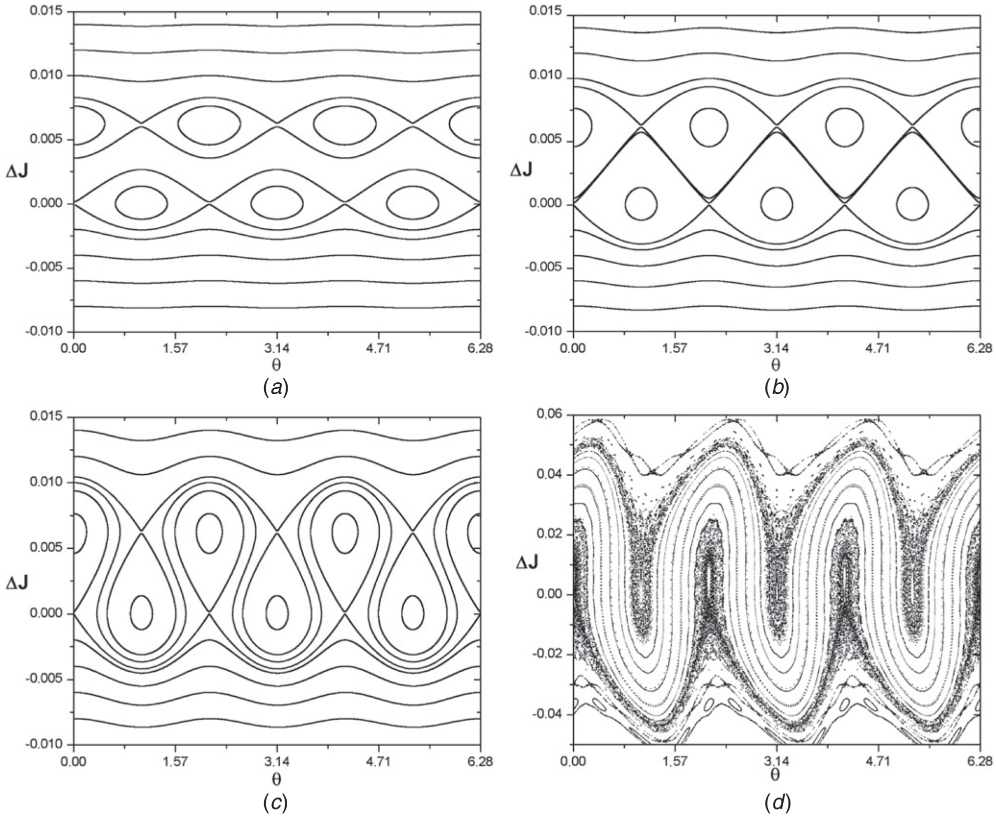

Figure 1. Map without robust tori from equations (14). (*a*) $\varepsilon = 2.0 \times 10^{-6}$: two independent isochronous resonances; (*b*) $\varepsilon = 0.5 \times 10^{-6}$: the reconnection process is starting; (*c*) $\varepsilon = 1.0 \times 10^{-5}$: the islands are dimerized; (*d*) $\varepsilon = 4.0 \times 10^{-3}$: neither chaos nor the invariant curves are limited by RT. The reader should observe the phase-space scale.

The associated equations for the discrete variables are equations (4) and (7) and based on equations (11) above we obtain

$$\begin{aligned} f(\Delta J_{n+1}, \theta_n) &= m_0\left(\Delta J_{n+1}^2 - a\right)\sin(m_0\theta_n), \\ g(\Delta J_{n+1}, \theta_n) &= 2\Delta J_{n+1}\cos(m_0\theta_n). \end{aligned} \tag{12}$$

Thus, with the perturbation period $T = \frac{2\pi}{N_r}$, we generate the following map satisfying equations (4):

$$\begin{aligned} \Delta J_{n+1} &= \Delta J_n + \varepsilon m_0\left(\Delta J_{n+1}^2 - a\right)\sin(m_0\theta_n), \\ \theta_{n+1} &= \theta_n + \frac{2\pi}{N_r}\left(\Delta J_{n+1} - \beta\Delta J_{n+1}^2\right) + 2\,\varepsilon\Delta J_{n+1}\cos(m_0\theta_n). \end{aligned} \tag{13}$$

This map expressed by equations (13) is our goal and we call it *non-twist standard map with robust tori (NTRT)*. We emphasize that from the theoretical point of view it is possible to introduce as isochronous resonances and robust tori as desired.

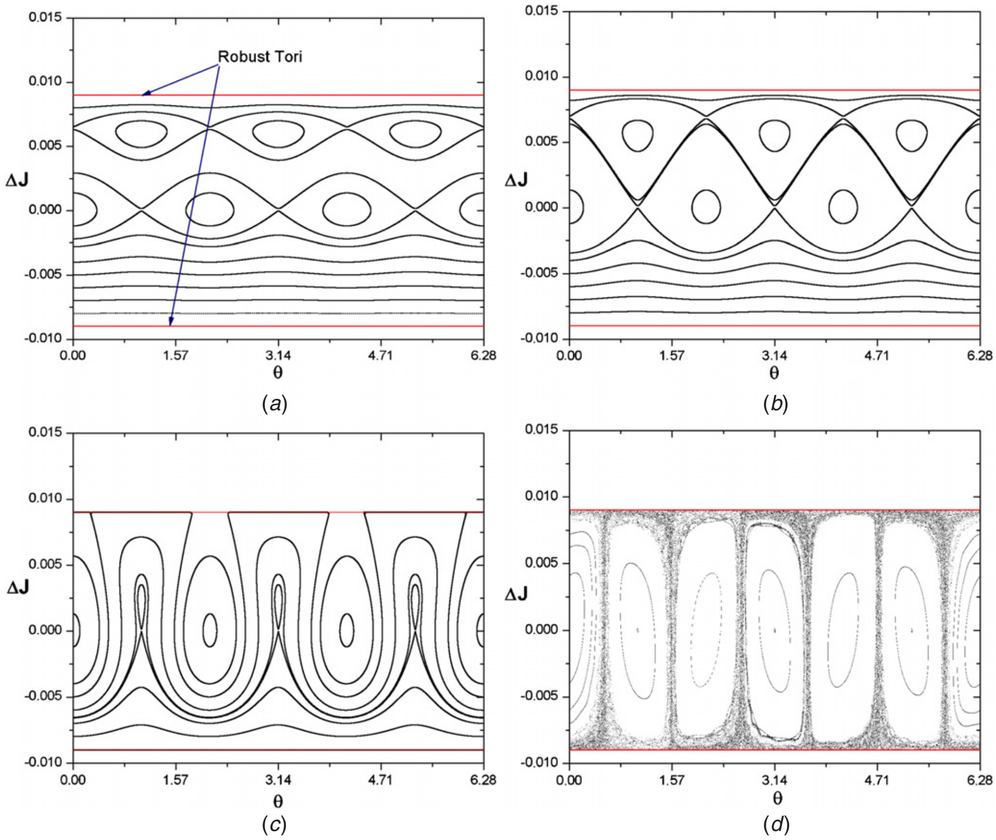

Figure 2. Map with robust tori from equations (13). (*a*) $\varepsilon = 3.0 \times 10^{-2}$: two non-interacting isochronous resonances with two RT; (*b*) $\varepsilon = 8.4 \times 10^{-2}$: the resonance chains are limited by the upper robust torus; (*c*) $\varepsilon = 4.9 \times 10^{-1}$: after reconnection, the dimerized islands are cut by the upper robust torus; (*d*) $\varepsilon = 20$: the chaotic magnetic field lines are confined in the region limited by RT. They are scattered back by RT or trapped by the small islands near RT.

Next, in order to put in evidence the effect of RT, we present two sets of plots, one without RT, whose non-twist map is the usual map

$$\begin{aligned} \Delta J_{n+1} &= \Delta J_n + \varepsilon m_0 \sin(m_0\theta_n), \\ \theta_{n+1} &= \theta_n + \frac{2\pi}{N_r}\left(\Delta J_{n+1} - \beta\Delta J_{n+1}^2\right), \end{aligned} \tag{14}$$

and another one with two RT, from equations (13). Figures 1(*a*)–(*c*) correspond to the usual map and they show two isochronous island chains non-interacting (*a*), reconnecting (*b*) and dimerized (*c*) as the control parameter ε is increased. Due to the non-KAM behaviour of the isochronous islands, the chaotic sea is not visible in the scale of the plots even though the non-twist standard map is non-integrable. On the other hand, in figure 1(*d*), a very strong perturbation is applied in order to show the change of the phase-space scale, as chaos and the invariant curves are not limited by RT.

Now, considering the map given by equations (13), we observe the birth of two straight lines (in red) corresponding to the RT previously cited, located at $\Delta J = \pm\sqrt{a}$. Looking at the Hamiltonian of equation (10) we observe that the perturbation is algebraically null at these values of ΔJ as already mentioned. When $\Delta J_{n+1} = \Delta J_n = \pm\sqrt{a}$ from equation (13), it means that the near-action is constant at these values of ΔJ, for any value of ε, defining the RT. In figure 2(*a*) we also see the two isochronous island chains far from each other, while in figure 2(*b*) they are reconnecting and in figure 2(*c*) the dimerized chains are cut by the RT located at $\Delta J = \sqrt{a}$. This means that, in this case with RT, the magnetic field lines will stop on the infinite barrier and the tokamak wall will not be attained. Figure 2(*d*) corresponds to a plot with a very strong perturbation only to put in evidence the role of RT when the chaotic sea is wider than in the other plots of figure 2. We can observe that the magnetic field lines are scattered back by both RT and they remain confined in the region limited by these RT. In a minor scale there are some small islands trapping the magnetic field lines because in the neighbourhood of these islands there is some stickiness. In all plots of figure 2, we have used $a = 8.1 \times 10^{-5}$.

4. Conclusions

In the approach we have presented here, the system (Hamiltonian and map) has only one resonant mode of non-KAM nature. Even though the dynamics of the magnetic lines, inside the chamber of the tokamak, present much instability making the experimental realization of robust tori (RT) difficult as it was conceived, the concept that they bring certainly improves the theoretical strategies for plasma confinement in tokamaks presented up to now because our map has all nonlinear dynamical ingredients of the typically used maps and it also has the robust barriers. Another relevant point to be emphasized is that, as the perturbations are null over RT by an exigency of continuity, in the neighbourhood of RT they are smaller than far from them, so these regions around RT will scatter back, or will trap, the magnetic lines which pass close to them. This point will be presented in a future paper.

We evaluate that an experimental realization of RT could be possible by considering a current in external coils, ergodic magnetic limiters (EML), that creates a magnetic resonance (n:m) at the peripheral region of the tokamak. Next, another perturbing magnetic field created by other coils could be superposed to the first one in order to create in a plasma region the same resonance (n:m) but now with an opposite magnetic field. With this setup, we suppose that each resonance cancels the effect of the other and a magnetic surface may locally emerge playing the role of RT. This modified equilibrium may have magnetic surfaces that reduce the plasma–wall interaction improving the plasma confinement.

We suggest a theoretical method to create transport barriers (robust tori) to avoid plasma–wall interactions. Thus, to create such barriers, we need to add a perturbation that, combined with the original one, gives rise to a modified perturbation vanishing in a determined position. The challenge is to perturb the plasma in a proper way to obtain this desired effect. In the following comment, we argue that the possibility mentioned in the paper is plausible. Thus, let us discuss this within two points of view. First, in our theoretical approach presented in this paper we propose to create a local barrier for the plasma transport through the elimination of the perturbations in a particular position. We emphasize that this is a local effect which is valid for any perturbation. Second, from the experimental point of view it is usual to have a reasonable control of the main mode of the perturbation (in this case the mode 1:3) whereas the control of the secondary modes in general is a difficult or even an impossible job. Hence, our conjecture to apply a second perturbation, from another set of EML with inverse magnetic field, infers that a robust barrier will appear locally where there was the main perturbation mode.

Finally, we conjecture that our map describes an effect that can significantly increase the plasma confinement time for controlled thermonuclear fusion.

Acknowledgments

The authors thank the Brazilian scientific agencies FAPESP and CNPQ for financial support.

References

[1] Horton W 1999 *Rev. Mod. Phys.* **71** 735
[2] Spatschek K H 2008 *Plasma Phys. Control. Fusion* **50** 124027
[3] Balescu R 2005 *Aspects of Anomalous Transport in Plasmas* (Bristol: Institute of Physics Publishing)
[4] Borgogno D, Grasso D, Pegoraro F and Schep T J 2008 *Phys. Plasma* **15** 102308
[5] Lichtenberg A J and Lieberman M A 1983 *Regular and Stochastic Motion* (New York: Springer)
[6] Hidalgo C *et al* 2005 *Nucl. Fusion* **45** S266
[7] Schaffer M J, Menard J E, Aldan M P, Bialek J M, Evans T E and Moyer R A 2008 *Nucl. Fusion* **48** 024004
[8] Finken K H, Evans T E, Reiter D, Spatschek K H and Suttrop W 2008 *Nucl. Fusion* **48** 020201
[9] Levinton F M *et al* 1995 *Phys. Rev. Lett.* **75** 4417
[10] Strait E J *et al* 1995 *Phys. Rev. Lett.* **75** 4421
[11] Mazzucato E *et al* 1996 *Phys. Rev. Lett.* **77** 3145
[12] Dreval M, Xiao C, Trembach D, Hirose A, Elgriw S, Pant A, Rohraff D and Niiu T 2008 *Plasma Phys. Control. Fusion* **50** 095014
[13] Marcus F A, Caldas I L, Guimaraes-Filho Z O, Morrison P J, Horton W, Kuznetsov Y K and Nascimento I C 2008 *Phys. Plasma* **15** 112304
[14] Chandre C, Ciraolo G, Doveil F, Lima R, Macor A and Vittot M 2005 *Phys. Rev. Lett.* **94** 074101
[15] Chandre C, Vittot M, Ciraolo G, Ghendrih P and Lima R 2006 *Nucl. Fusion* **46** 33
[16] Voyatzis G and Ichtiaroglou S 1999 *Int. J. Bifurcation Chaos* **9** 849
[17] Egydio de Carvalho R and Favaro G M 2005 *Physica* A **350** 173
[18] Egydio de Carvalho R, Martins C G L and Favaro G M 2009 *Braz. J. Phys.* **39** 606
[19] Kucinski M Y and Caldas I L 1987 *Z. Naturforsch.* A **42** 1124
[20] Portela J S E, Caldas I L and Viana R L 2008 *Eur. Phys. J. Spec. Top.* **165** 195
[21] Abdullaev S S 2006 *Construction of Mappings for Hamiltonian Systems and Their Applications* (New York: Springer)
[22] Roberto M, da Silva E C, Caldas I L and Viana R L 2004 *Phys. Plasma* **11** 214
[23] Karger F and Lackner F 1977 *Phys. Lett.* A **61** 385
[24] Engelhardt W and Feneberg W 1978 *J. Nucl. Mater.* **76** 518
[25] Kerner W and Tasso H 1982 *Phys. Rev. Lett.* **49** 654
[26] Morrison P J 2000 *Phys. Plasma* **7** 2279
[27] Portela J S E, Caldas I L, Viana R L and Morrison P J 2007 *Int. J. Bifurcation Chaos* **17** 1589
[28] del Castillo-Negrete D and Morrison P J 1993 *Phys. Fluids* A **5** 948
[29] Egydio de Carvalho R and Ozório de Almeida A M 1992 *Phys. Lett.* A **162** 457
[30] Egydio de Carvalho R 1993 *Nonlinearity* **6** 973
[31] del Castillo-Negrete D, Greene J M and Morrison P J 1996 *Physica* D **91** 1
[32] Wurm A, Apte A, Fuchss K and Morrison P J 2005 *Chaos* **15** 023108
[33] McCauley J L 1988 *Phys. Scr.* **T20** 5
[34] Percival I and Richards D 1982 *Introduction to Dynamics* (New York: Cambridge University Press)